

## Glueballs and topology with $\mathcal{O}(a)$ -improved lattice QCD.

UKQCD and QCDSF Collaborations: A. Hart<sup>a</sup>

<sup>a</sup>DAMTP, Cambridge University, Wilberforce Road, Cambridge CB3 0WA, UK.

We present evidence for unquenching effects in  $N_f = 2$ ,  $16^3 32$  ensembles by comparing with ‘equivalent’ quenched data at  $\hat{r}_0 \simeq 5.0$ . A (small) VEV for torelons signals (weak) string breaking. A 15 – 20% reduction in the scalar glueball mass relative to quenched is argued to be (in part at least) a discretisation effect. We find a chiral suppression of the topological susceptibility consistent with expectations, and agreement between fermionic and gluonic methods for measuring the topological charge.

To study the effects of vacuum polarisation in QCD, we should vary the sea quark mass,  $m_q$ , having first removed discretisation effects. With confident continuum extrapolations of many lattice quantities unavailable, however, we must instead try to ‘freeze’ lattice artefacts. UKQCD does this by attempting to fix the lattice Sommer scale,  $\hat{r}_0 \simeq 5$ , as  $m_q$  is changed. Variations due to residual changes in  $\hat{r}_0$  are further reduced by the the leading order discretisation errors for the  $\mathcal{O}(a)$ -improved action being quadratic, rather than linear, in the lattice spacing,  $a$ . An ‘equivalent’ value of  $\hat{r}_0$  is found in the quenched, ‘gluodynamical’ theory at coupling  $\beta_{\text{Wil}} = 5.93$ . Details of scales, parameters and matching can be found in [1]. We use as a measure of  $m_q$  the square of the pseudoscalar ‘pion’ mass. Circumflexes denote dimensionless lattice quantities.

The failure of experiments to detect unambiguous glueball states is believed to be a consequence of mixing between the light glueballs and  $q\bar{q}$  states. A major goal of lattice QCD is to predict the mixing matrix elements, but the uncertainties in attempts so far [2,3] mean, however, that phenomenological attempts to describe the content (gluonic or  $q\bar{q}$ ) of the scalar sector glueball candidates lead to widely differing results [4].

As a preliminary to a full mixing analysis [5], we study the light glueballs and winding flux tubes on UKQCD dynamical configurations and find, in common with [6], that accurate mass estimates are possible on moderately sized ensembles (4000 – 8000 HMC trajectories). Full results can

be found in [7], along with a discussion of the applicability of the term ‘glueball’ when mixing is induced by vacuum polarisation.

On a spatial torus, Polyakov loops (PL) couple to colour flux tubes that close upon themselves through the periodic boundary with unit winding number. In the confining phase of gluodynamics such ‘torelons’ are stable, with the PL vacuum expectation value (VEV) zero even after operator improvement. To a first approximation the flux tube mass is the product of the string tension,  $\hat{K}$ , and the spatial extent of the lattice,  $L$ .

Dynamical quarks break the centre symmetry that ensures the orthogonality of contractible and non-contractible operators. The PL can now have a non-zero VEV. This VEV should increase as  $m_q \rightarrow 0$  (and centre symmetry breaking gets worse) and, due to the spatially periodic fermionic boundary conditions, be negative. In a simple model it goes as  $-(m_q)^{-L}$  for (moderately) heavy sea quarks [7]. This is ‘string breaking’ of the confining flux tube, and Fig. 1 confirms this picture for improved PL VEVs. With the breaking of centre symmetry, mixings between torelons winding in different directions becomes possible. Also allowed is mixing between single (non-contractible) PL and (contractible) glueball operators. This should be the leading source of (mass reducing) finite volume effects in the scalar glueball: the double torelon that plays this rôle in the quenched theory is too heavy to figure here. Both mixings are very weak, however, as expected for a numerically small VEV, and we can be con-

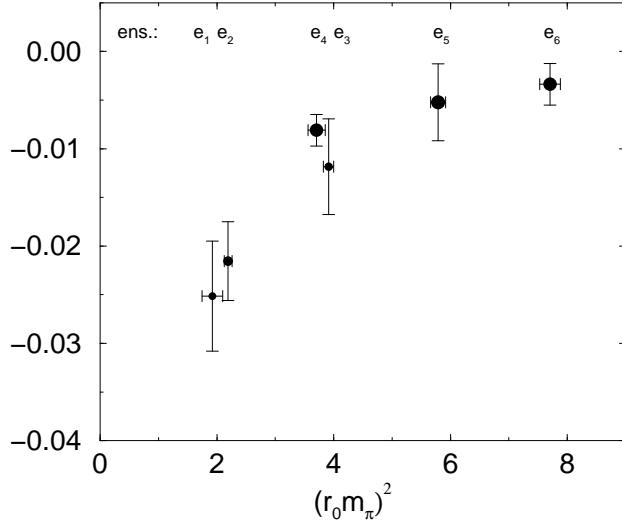


Figure 1. The VEV of the spatial torelon.

ident that finite volume effects are small for the scalar glueball. We can also thus use the torelon mass to obtain  $\hat{K}$ , which agrees well with that from static interquark potential fits [1].

The masses of the lightest scalar and tensor states are shown in Fig. 2, with the ‘equivalent’ quenched results at  $\beta_{\text{Wil}} = 5.93$ , and the threshold for the scalar to decay to pseudoscalars. Whilst the (admittedly noisy) tensor mass shows no significant quenching effect, vacuum polarisation reduces the scalar mass by 15 – 20%. The at most weak dependence of this figure on  $m_q$  and the  $\pi\pi$  threshold suggest it is an increased discretisation effect relative to the quenched theory, and that it may not persist in the continuum limit. In gluodynamics, this ‘scalar dip’ is (probably) due to the scaling trajectory,  $\beta_{\text{Wil}} \rightarrow \infty$ , passing close to a critical point in the extended fundamental–adjoint gauge coupling plane. The further reduction in the presence of sea quarks for the  $\mathcal{O}(a)$ –improved action is then not unexpected: hopping parameter expansions suggest the scaling trajectory now passes even closer to this critical point. Measurements of the couplings in such a mixed effective action appear to support this. The lessened scalar mass at fixed, finite  $a$  is thus not necessarily indicative of a continuum effect [8].

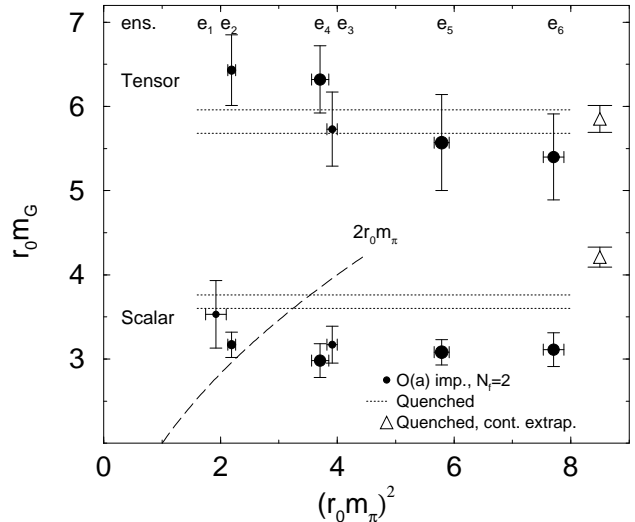


Figure 2. The lightest glueball masses.

The ability to vary parameters fixed in Nature has made lattice Monte Carlo simulation a valuable tool for investigating the rôle of topological excitations in QCD and related theories.

The topological susceptibility,  $\chi = \langle Q^2 \rangle / V$ , is the squared expectation value of the topological charge,

$$Q = \frac{1}{32\pi^2} \int d^4x \frac{1}{2} \varepsilon_{\mu\nu\sigma\tau} F_{\mu\nu}^a(x) F_{\sigma\tau}^a(x) \quad (1)$$

normalised by the volume. Sea quarks induce an instanton–anti-instanton attraction which becomes stronger in the continuum limit, suppressing  $\chi$  [11]. Given various assumptions [12], in the chiral limit of  $N_f$  flavours we have  $\chi = f_\pi^2 m_\pi^2 / (2N_f) + \mathcal{O}(m_\pi^4)$ . This is in a convention where the experimental value of the pion decay constant  $f_\pi \simeq 93$  MeV, and requires  $f_\pi^2 m_\pi^2 V \gg 1$ , which holds for the lattices used here. The topological susceptibility is measured on UKQCD gauge fields using a symmetrised ‘Wilsonian’ operator,  $\hat{Q}(n)$ , having first performed 10 Wilson action cools to regulate the ultraviolet dislocations. Fig. 3 shows the chiral suppression in  $\hat{\chi}$  relative to the quenched limit with an interpolating fit [9]. Including the  $m_\pi^4$  term, we can fit the four most chiral data, obtaining  $f_\pi = 105 \pm 6 \pm_{-10}^{+18}$  MeV at  $a \simeq 0.1$  fm. A fuller discussion of these results is

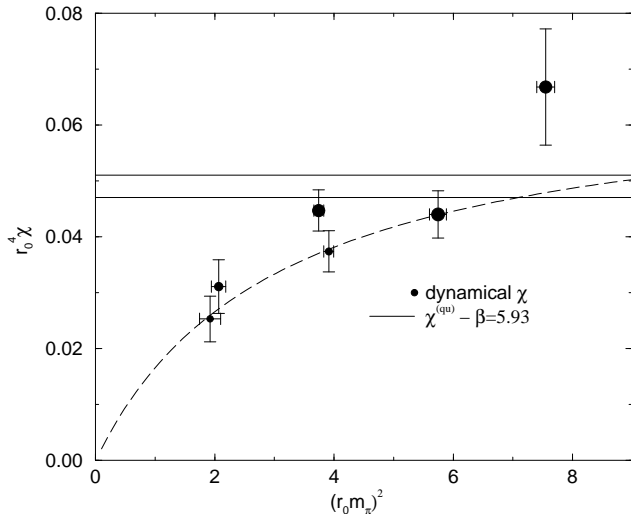


Figure 3. The topological susceptibility.

available in [9,10].

The topology of the vacuum is clearly influenced by the sea quarks. At finite  $a$ , however,  $\hat{Q}$  is method dependent. To understand the systematic biases this introduces, we compare several contrasting methods with differing systematic errors for measuring  $\hat{Q}$  on a QCDSF ensemble for  $a \simeq 0.1$  fm. The first is as described above. We also use the ‘5Li’ method [13], which is exact up to  $\mathcal{O}(a^6)$  and approximately restores scale invariance for large lattice instantons. We use the Boulder smearing technique, which mimics a renormalisation group inspired smoothing of the gauge fields [14]. Finally, we employ a fermionic charge operator on the ‘hot’ gauge fields [15].

Fig. 4 shows Monte Carlo time series of the various  $\hat{Q}$ , which have not been rounded to the nearest integer. We can quantify the visually striking agreement through normalised correlation functions using pairs of measurements. Preliminary results give 85–95% agreement between any pair of charge definitions; subsequent work will compare systematic effects and the statistical accuracy of topological susceptibility measurements. Other work in this area can be found in [16].

We thank Ph. de Forcrand for access to his code, and T. Kovacs and D. Pleiter for results used in Fig. 4.

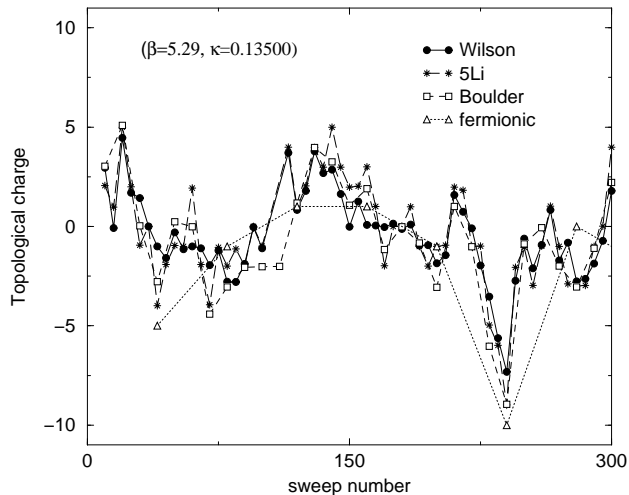


Figure 4. Comparing topological charges.

## REFERENCES

1. C. Allton et al., hep-lat/0107021.
2. D. Toussaint, Nucl. Phys. (PS) 83-84 (2000) 151 [hep-lat/9909088].
3. C. Michael et al., Nucl. Phys. (PS) 83-84 (2000) 185 [hep-lat/9909036]; C. McNeile, C. Michael, Phys. Rev. D 63 (2001) 114503 [hep-lat/0010019].
4. F. Close, A. Kirk, hep-ph/0103173.
5. C. Michael, C. McNeile, A. Hart, M. Teper, in progress.
6. G. Bali et al., Phys. Rev. D 62 (2000) 054503 [hep-lat/0003012].
7. A. Hart, M. Teper, hep-lat/0108022.
8. A. Hart, preprint DAMTP-2001-75.
9. A. Hart, M. Teper, hep-lat/0108006.
10. A. Hart, M. Teper, hep-ph/0004180; hep-lat/0009008; Nucl. Phys. B (PS) 83-84 (2000) 476 [hep-lat/9909072].
11. P. Di Vecchia, G. Veneziano, Nucl. Phys. B 171 (1980) 253.
12. H. Leutwyler, A. Smilga, Phys. Rev. D 46 (1992) 5607.
13. Ph. de Forcrand et al., Nucl. Phys. B 499 (1997) 409 [hep-lat/9701012].
14. T. DeGrand, A. Hasenfratz, T. Kovacs, Nucl. Phys. B 520 (1998) 301 [hep-lat/9711032].
15. D. Pleiter, Proceedings of Lattice01.
16. B. Alles et al., Phys. Rev. D 58 (1998) 071503 [hep-lat/9803008].

**Acknowledgments.**

We thank the United Kingdom PPARC for support via the UKQCD research and travel grants, and for postdoctoral funding.